

8th International Conference on Porous Metals and Metallic Foams, Metfoam 2013

Advanced fabrication of nanoporous Ni-based superalloy membranes

Björn Hinze*, Joachim Rösler

Institute for Materials, TU Braunschweig, Langer Kamp 8, Braunschweig D-38106, Germany.

Abstract

Nickel-based superalloys are predominantly used as structural materials in high-temperature applications due to their exceptional high-temperature strength resulting from precipitation hardening of the coherent γ' -phase. The self-assembly of the γ' -cubes to interconnected networks can be utilized by electrochemical leaching to produce nanoporous superalloy membranes with open porosity and, therefore, functional properties. So far, only γ' -membranes consisting of the intermetallic compound $\text{Ni}_3(\text{Al}, \text{Ti}, \text{Ta})$ have been manufactured and analyzed. In this work, the production of the mirrored γ -membranes, consisting of the nickel solid solution, is described.

© 2014 Published by Elsevier Ltd. This is an open access article under the CC BY-NC-ND license (<http://creativecommons.org/licenses/by-nc-nd/3.0/>).

Peer-review under responsibility of Scientific Committee of North Carolina State University

Keywords: Dendrites; Coarsening; Self-Assembly; CMSX-4; Mechanical Behavior; Fracture Surface; Phase Extraction.

1. Introduction

Open-pored metals are modeled and developed due to their functional properties (Golosnoy et al. (2008), Xie et al. (2004), Rösler and Mukherji (2005), Lefebvre (2008)). Pore size and porosity result from the production processes like sintering of metal fibers (Golosnoy et al. (2008)), coating of polymer foams (Paserin et al. (2004)), melt infiltration techniques (Brothers et al. (2005)) or selective phase extraction (Rösler and Mukherji (2005), Rösler et al. (2005), Rösler and Nāth (2010), Hinze et al. (2011)). The selective phase extraction allows the production of membranes with pore sizes of several hundred nanometers and a porosity of around 50%. In this work, the Ni-based superalloy CMSX-4 was used. The exceptional high-temperature strength of this alloy results from precipitation hardening of cubic precipitates of the coherent γ' -phase in the nickel solid solution or γ -phase. Due to the γ/γ' -lattice

* Corresponding author. Tel.: +49-531-391-3062; fax: +49-531-391-3058.

E-mail address: b.hinze@tu-bs.de

misfit and the high γ' -volume fraction, the cubic γ' -precipitates align parallel to the $\langle 001 \rangle$ directions of the crystal lattice. During heat treatment at high temperatures, the γ' -particles coarsen directionally generating an interpenetrating network of γ and γ' . This process is driven by diffusion and internal stress fields, caused by solidification and segregation during the casting process (Epishin et al. (2004)). To produce nanoporous membranes with channel-like interconnected pores, either the γ or the γ' -phase can be extracted selectively from the interpenetrated network. In the following, the production of γ -membranes, consisting of the nickel solid solution, is described. The mechanical properties of the membranes are discussed using stress-strain curves. Furthermore, the fracture surfaces are analyzed using scanning electron microscopy (SEM) images.

2. Experimental

The material used in this study is a single crystalline plate of the Ni-based superalloy CMSX-4, which was cast in a Bridgman process. The chemical composition in wt.% is 5.52 Al, 9.46 Co, 6.56 Cr, 0.1 Hf, 0.61 Mo, 2.99 Re, 6.57 Ta, 1.00 Ti, 6.45 W and the balance is Ni. As a result of the solidification process, the microstructure is dendritic. The direction of growth of the primary dendrites is along the $[001]$ direction which is also the longitudinal direction of the plate. Note, that there can be a slight angular tilt between these two directions which is neglected in this work. The area perpendicular to the longitudinal direction is built by the short and long transverse direction of the single crystal plate, see Fig. 1. The dendritic solidification also causes an inhomogeneous distribution of elements due to segregations. To homogenize the material, the first heat treatment consists of the following steps: 1550K/2h, 1561K/3h, 1569K/3h, 1577K/2h, 1586K/2h, 1589K/2h, 1591K/2h, and 1594K/2h. However, complete homogenization is not possible due to the high amount of refractory elements like W or Re which are enriched in dendrites. Consequently, the dendritic microstructure is still apparent causing internal stress fields. The so-called dendritic stress is the driving force for directional coarsening (Epishin et al. (2004)) which can be used to produce an interpenetrated network of γ and γ' (Hinze et al. (2011)). The coarsening process is diffusion driven but the γ' -volume fraction also changes with the processing temperature. The higher the temperature, the smaller is the γ' -volume fraction but the faster is the diffusion process. In this study, the γ/γ' -network was generated in a second heat treatment at 1353K for 1000h. At this temperature, the ThermoCalc software predicts using the TTNi7 database around 50.0% γ' , 48.5% γ and 1.5% μ which is a topologically close packed (TCP) phase. These phases were also experimentally observed by (Cheng et al. (2011)). The fully annealed plate was cut into sheets which were ground on both sides to a thickness of about 250 μ m. The γ' -phase was selectively extracted using electrochemical leaching in a potentiostatic cell using a potential of 0.275V and an ethanol or methanol based electrolyte containing 0.50% citric acid and 0.75% hydrogen chloride (Näth (2008)). Finally, the mechanical properties of the membranes were analyzed using a tensile testing machine. In this work, three different combinations of membrane surface orientation and direction of tensile testing were analyzed, compare also Fig. 1: (i) surface: longitudinal x short transverse and tensile testing along longitudinal (lt-l), (ii) surface: longitudinal x short transverse and tensile testing along short transverse (lt-t), and (iii) surface: short transverse x long transverse and tensile testing along long transverse (tt-t). Note, that the orientation of the primary dendrites is along the $[001]$ direction which is also the longitudinal direction of the plate and that long and short transverse directions are both perpendicular to the primary dendrites.

3. Results

The stress-strain curves of the three different membranes are shown in Fig. 2. The mechanical properties vary for the different membranes and depend on the combination of membrane orientation and direction of the tensile testing. The tt-t membranes have the highest strength of up to 35MPa. Note, that the porosity was neglected and all values refer to the total cross-section of the tested specimen. The lt-t membranes reach stress values of up to 20MPa, whereas, the lt-l membranes just reach stress values of around 10MPa.

In Fig. 3, SEM images of the membrane surfaces close to the fracture and the fracture surfaces of the three different membrane types are displayed. In Fig. 3a and 3b, the tt-t membrane is shown. The dendritic structure can be seen as cross in Fig. 4a. The fracture surface goes around the dendrites and is wavy. Fig. 3c and 3d show the lt-t membrane. Here, the fracture surface proceeds almost straight through the material and is just slightly tortuous. In the fracture surface, the γ -phase morphology is mainly plate-like. In Fig. 3e and 3f, the lt-l membrane is displayed.

The fracture runs straight through dendritic and interdendritic regions. In Fig. 3e, a dendritic region can be seen in the upper third due to the apparent μ -phase needles, whereas, a interdendritic region can be seen in the lower third due to the coarser membrane structure. In the fracture surface, the γ -phase morphology is mainly plate-like.

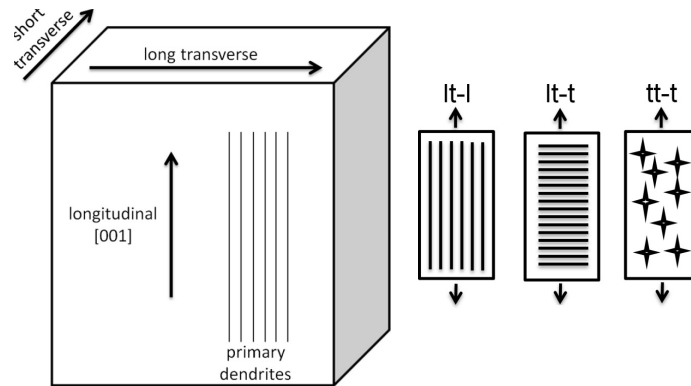


Fig. 1. Nomenclature of directions in the used plate (left) and combinations of membrane surface orientation and direction of tensile testing (right).

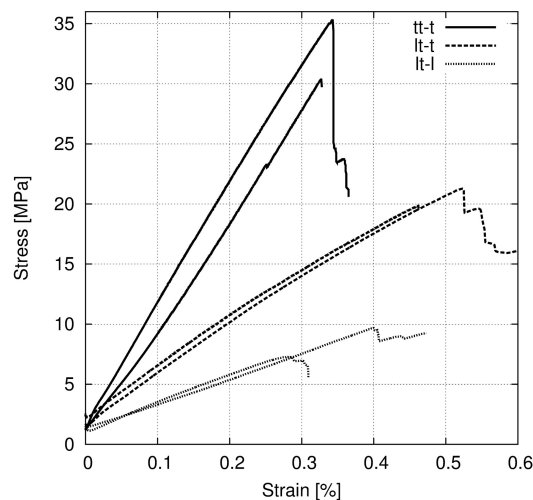


Fig. 2. Stress-strain curves of the tested membranes.

4. Discussion

The higher strength of the tt-t membranes is caused by the orientation of the γ -plates since the plates are usually not perpendicular to the fracture surface. Consequently, there are more connections in the direction of tensile stress which strengthens the membrane in this direction. The low strength of the lt-l membranes is caused by the opposite phenomena. In dendritic and interdendritic regions, the γ -plates are oriented perpendicular to the direction of tensile stress. Consequently, the number of interconnections between the plates is reduced and the material strength is reduced. In lt-t membranes, the γ -plates in the fracture surface are mainly oriented perpendicular to the direction of tensile testing, resulting in a material strength in between the one of tt-t and lt-l membranes. This can also be observed in the fracture path which is slightly tortuous in lt-t membranes but not as wavy as in tt-t membranes or as straight as in lt-l membranes. Furthermore, the μ -phase can be seen in dendritic regions because this topologically closed packed (TCP) phase contains Re and W which segregate dendritically. Around the μ -phase, the γ -phase dissolves during the electrochemical leaching probably because the matrix is depleted of chromium.

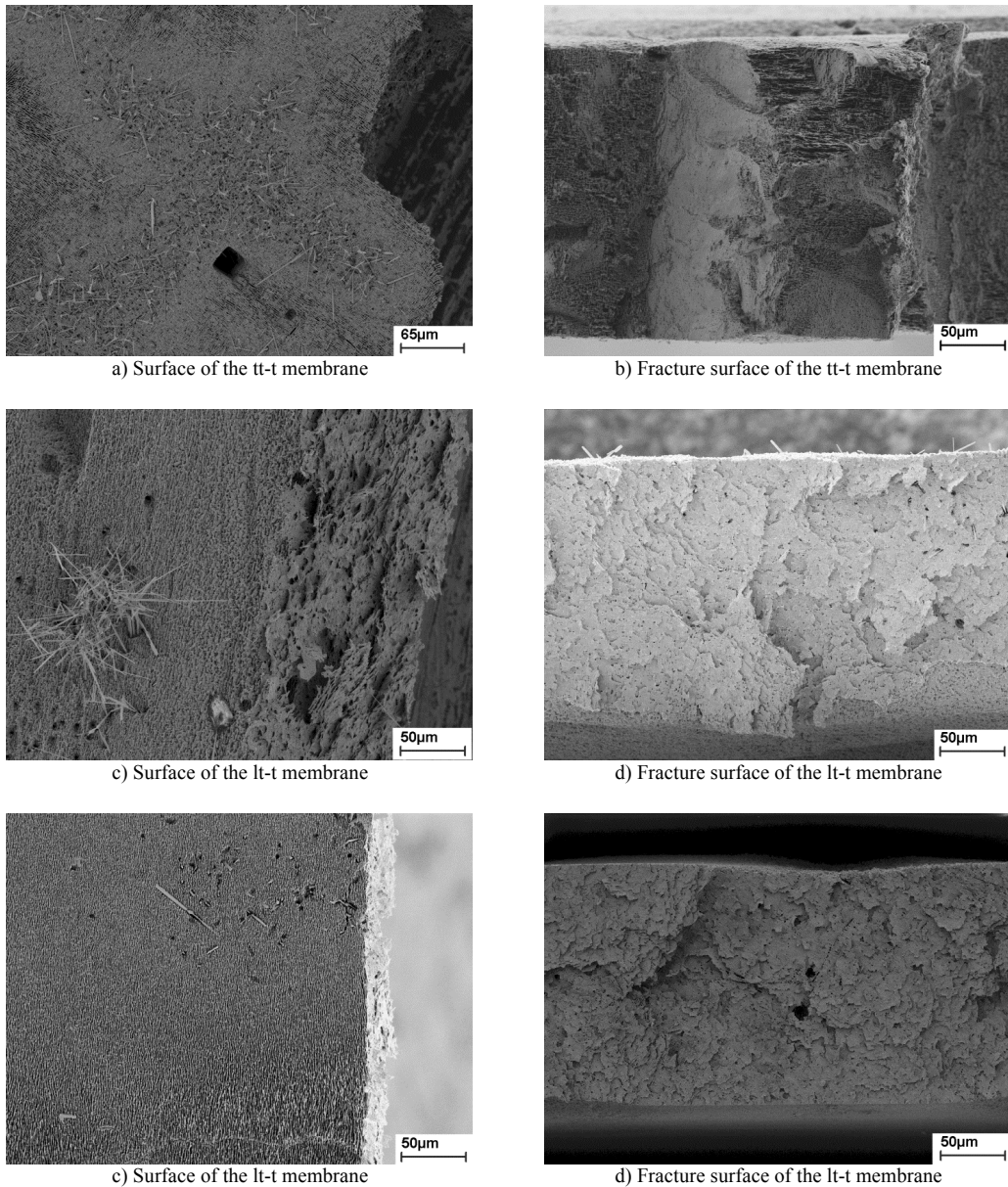


Fig. 3. Membrane surfaces close to the fracture (left) and fracture surfaces of the tested membranes (right).

5. Conclusion

It has been demonstrated that nanoporous γ -membranes can be produced by selectively extracting the γ' -phase in an alcoholic electrolyte. Finally, the following key findings can be outlined: (i) The TCP phase μ is not extracted using electrochemical leaching and is still apparent; (ii) the γ -membranes have a plate-like structure; (iii) the orientation of the plates is highly dependent on the dendritic microstructure. The lowest material strength results when a fracture path is available where the γ -plates are oriented perpendicular to the applied tensile stress. This is

achieved when the tensile stress is applied in longitudinal direction, i.e. the direction of growth of the primary dendrites.

Acknowledgements

Financial support provided by research program *Bürgernahe Flugzeug* of the German federal state of Lower Saxony is gratefully acknowledged.

References

- Brothers, A.H., Scheunemann, R., DeFouw, J.D., Dunand, D.C., 2005. Processing and structure of open-celled amorphous metal foams. *Scripta Materialia* 52, 335–339.
- Cheng, K.Y., Jo, C.Y., Jin, T., Hu., Z.Q., 2011. Precipitation behaviour of μ phase and creep rupture in single crystal superalloy CMSX-4. *Journal of Alloys and Compounds* 509, 7078–7086.
- Epishin, A., Link, T., Brückner, U., Fedeliche, B., Portella, P., Green, K.A., Pollock, T.M., Harada, H., Howson, T.E., Reed, R.C., Schirra, J.J., Walston, S., (Eds.). 2004. Effects of segregation in nickel-base superalloys: dendritic stresses. *Superalloys 2004*, TMS, 537–543.
- Golosnoy, I.O., Tan, J.C., Clyne., T.W., 2008. Ferrous Fibre Network Materials for Jet Noise Reduction in Aeroengines Part I: Acoustic Effects. *Advanced Engineering Materials* 10, 192–200.
- Hinze, B., Rösler, J., Schmitz, F., 2011. Production of nanoporous superalloy membranes by load-free coarsening of γ' -precipitates. *Acta Materialia* 59, 3049–3060.
- Lefebvre, L.-P., Banhard, J., Dunand., D.C., 2008. Porous Metals and Metallic Foams: Current Status and Recent Developments. *Advanced Engineering Materials* 10, 775–787.
- Näth, O. 2008. Nanoporöse Strukturen auf Nickelbasis, Cuvillier, Göttingen.
- Paserin, V., Marcuson, S., Shu, J., Wilkinson, D., 2004. CVD Technique for Inco Nickel Foam Production. *Advanced Engineering Materials* 6, 454–459.
- Rösler, J., Mukherji, D., 2003. Design of Nanoporous Superalloy Membranes for Functional Applications. *Advanced Engineering Materials* 5, 916–918.
- Rösler, J., Näth, O., 2010. Mechanical behaviour of nanoporous superalloy membranes. *Acta Materialia* 58, 1815–1828.
- Rösler, J., Näth, O., Jäger, S., Schmitz, F., Mukherji, D., 2005. Fabrication of nanoporous Ni-superalloy membranes. *Acta Materialia* 53, 1397–1406.
- Xie, Z., Ikeda, T., Okuda, Y., Nakajima, H., 2004. Sound absorption characteristics of lotus-type porous copper fabricated by unidirectional solidification. *Material Science Engineering A* 386, 390–395.